

# One-dimensional quantum walks driven by two entangled coins

S. Panahiyan<sup>1,2,3</sup> \* and S. Fritzsche<sup>1,2,3†</sup>

<sup>1</sup>*Helmholtz-Institut Jena, Fröbelstieg 3, D-07743 Jena, Germany*

<sup>2</sup>*GSI Helmholtzzentrum für Schwerionenforschung, D-64291 Darmstadt, Germany*

<sup>3</sup>*Theoretisch-Physikalisches Institut, Friedrich-Schiller-University Jena, D-07743 Jena, Germany*

We study a one-dimensional quantum walk with four internal degrees of freedom (two entangled qubits) driven by two entangled coins. We will demonstrate that the entanglement, introduced by the coins, enables one to steer the walker's state from a classical to standard quantum-walk behavior with two-dimensional coins, and to novel behaviour not found for one-dimensional walks otherwise. We also show that states with a symmetric density distribution and a maximum or minimum of the entropy are found only for maximally entangled initial states (Bell states). On the other hand, the type of probability density distribution and its variance are only determined by entangled coins. We will make contrast between cases where entangled coins are identical and non-identical, and show how the effective behavior of internal degrees of freedom bases would be different for these cases. In addition, we explain how the entanglement of two-qubit initial state determines the most probable place to find the walker.

## I. INTRODUCTION

Quantum walks (QW), i.e. walks driven by the laws of quantum mechanics, are known to behave very differently from their classical counterparts [1]. In contrast to classical walks (CW), QW may exhibit a ballistic spread for its probability density distribution (PDD). Therefore, QW have been found an efficient framework to develop new (quantum) algorithms [2], increase the processing power to solve computationally hard problems [3] and to simulate other quantum systems [4]. QWs are known also as universal computational primitives [5] and generators of PDD [6]. This makes them ideal for quantum simulation [7]. In addition, these walks were used to explore topological phases [8], build neural networks [9], prepare quantum states [10] and engineer them [11]. Experimentally, QW has been realized with ultracold atoms [12], photons [13], ions [14], Bose-Einstein condensate [15] and optical-network [16, 17]. In fact, one of the desirable features of QW is the possibility of demonstrating it by means of different systems.

Entanglement is another feature and resource of quantum systems with no classical counterpart [18]. This resource plays a crucial role in quantum information and its applications/protocols such as superdense coding [19], teleportation [20], cryptography [21], quantum computation [22] and algorithmic construction [23, 24]. For these reasons, there has been a growing interest to create entangled states and make them available for different applications [18]. Naturally, it is possible to use the entanglement as a resource in QWs as well.

In this paper, we consider a single walker with four internal degrees of freedom that moves within a one-dimensional position space. The four internal degrees of freedom are realized by two qubits that are initially en-

tangled with each other and are driven by two coin operators referred as *two entangled coins* in literature [25, 26]. Previously, only special cases of such walk were investigated and it was found that: These walks exhibit a persistent major peak at the initial position and two other distinguishable peaks at the extreme zones [25]. Also, the probability of finding the walker at any given location eventually becomes stationary and non-vanishing [26]. In this work, in contrast, we consider further and more general coins and initial states. In particular, we show: *I*) walkers with a rather diverse behavior including: Gaussian like, Two-, Three- and Four-peaks-zone. This makes entanglement between qubits a resource for introducing novel behaviors and obtain previously reported ones. *II*) Zero probability of finding the walker at specific locations when entangled coins are not identical. *III*) The dependency of walk's symmetries, the most probable place to find the walker and maximization (minimization) of its entropy on the amount of entanglement in initial state.

The structure of paper is as follows: first, we introduce the setup of the walk, its parameters and highlight some of its properties (II). Next, we simulate the walk for two scenarios governing the coin's structure with three different initial states. We investigate the properties of walker's behavior as a function of coin's and initial states' parameters (III). Then, we study the evolution of entropy and extract the conditions for its maximization (minimization) for different cases (IV). The paper is concluded with some closing remarks in section V.

## II. SETUP OF THE WALK

The walker is generally a quantum system that moves stepwise in position space due to its four internal degrees of freedom. Here, we represent the internal state of the walker by two entangled qubits. The Hilbert space of the coin (internal degrees of freedom),  $\mathcal{H}_C$ , is spanned by  $\{|00\rangle, |11\rangle, |10\rangle, |01\rangle\}$ . The coin operator of the walk is given by tensor product of two single-qubit coin

\*email address: shahram.panahiyan@uni-jena.de

†email address: s.fritzsche@gsi.de

operators (sub-coins),  $\hat{C} = \hat{C}_1 \otimes \hat{C}_2$  where

$$\hat{C}_1 = \cos \theta |0\rangle_C \langle 0| + \sin \theta |0\rangle_C \langle 1| + \sin \theta |1\rangle_C \langle 0| - \cos \theta |1\rangle_C \langle 1|, \quad (1)$$

$$\hat{C}_2 = \cos \gamma |0\rangle_C \langle 0| + \sin \gamma |0\rangle_C \langle 1| + \sin \gamma |1\rangle_C \langle 0| - \cos \gamma |1\rangle_C \langle 1|. \quad (2)$$

Both,  $\hat{C}_1$  and  $\hat{C}_2$  can be understood as rotation matrices that are characterized by their rotation angles,  $\theta$  and  $\gamma$ . The total coin operator is then obtained as

$$\begin{aligned} \hat{C} = & |00\rangle_C (\cos \theta \cos \gamma \langle 00| + \cos \theta \sin \gamma \langle 01| \\ & + \sin \theta \cos \gamma \langle 10| + \sin \theta \sin \gamma \langle 11|) + \\ & |01\rangle_C (\cos \theta \sin \gamma \langle 00| - \cos \theta \cos \gamma \langle 01| \\ & + \sin \theta \sin \gamma \langle 10| - \cos \theta \sin \gamma \langle 11|) + \\ & |10\rangle_C (\sin \theta \cos \gamma \langle 00| + \sin \theta \sin \gamma \langle 01| \\ & - \cos \theta \cos \gamma \langle 10| - \cos \theta \sin \gamma \langle 11|) + \\ & |11\rangle_C (\sin \theta \sin \gamma \langle 00| - \sin \theta \cos \gamma \langle 01| \\ & - \cos \theta \sin \gamma \langle 10| + \cos \theta \cos \gamma \langle 11|). \end{aligned} \quad (3)$$

Of course, it is possible to consider other coin operators instead of those given in Eqs. (1) and (2). Our choices of these sub-coins are due to their unitary nature. If  $\hat{C}$  acts upon the internal state of the walker, it generally results into a superposition of basis states. Fig. 1 shows schematically how such superposition is created for different initial states (Eqs. 6 - 8).

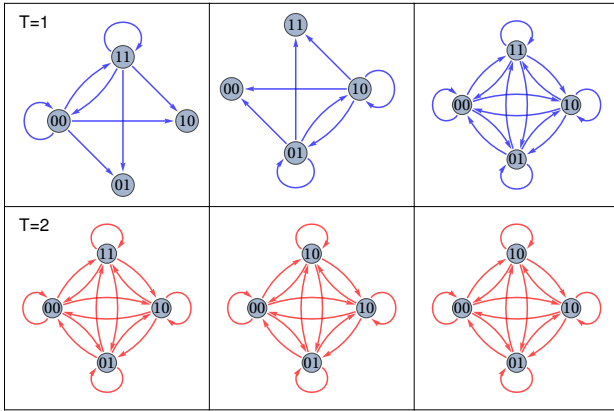


FIG. 1: Schematic plot for considered coin operator (3) in the first two subsequent steps for three initial states; Left column: Eq. (6), middle column: Eq. (7) and right column: Eq. (8).

The walker moves along a one-dimensional lattice where its Hilbert space,  $\mathcal{H}_P$ , is spanned by  $\{|i\rangle_P : i \in \mathbb{Z}\}$ . The conditional shift operator that moves the walker is given by

$$\begin{aligned} \hat{S} = & |00\rangle_C \langle 00| \otimes \sum |i+1\rangle_P \langle i| + \\ & (|10\rangle_C \langle 10| + |01\rangle_C \langle 01|) \otimes \sum |i\rangle_P \langle i| + \\ & |11\rangle_C \langle 11| \otimes \sum |i-1\rangle_P \langle i|. \end{aligned} \quad (4)$$

The internal degrees of freedom provide the possibility of including three types of movement for the walker: depending on internal degrees of freedom, the walker move to *right*, *left* or *remain* in the same position. This is schematically sketched in Fig. 2

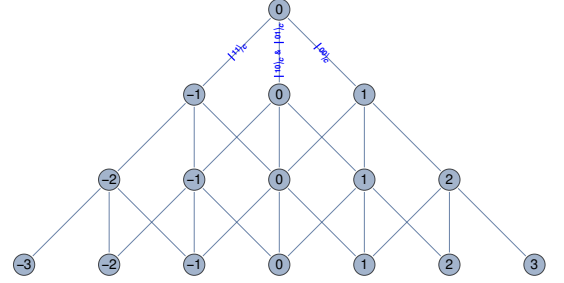


FIG. 2: Schematic plot for considered shift operator (4) in the first three subsequent steps.

In QW with two-dimensional coin space, PDD is non-zero in odd (even) positions for odd (even) steps. This is because the shift operator of walk has only two options; moving to right or left in each step. In contrast, for this walk, the third option is provided for the shift operator. This results into non-zero probability density for both odd and even positions in each step.

The Hilbert space of the walker is given by  $\mathcal{H} \equiv \mathcal{H}_P \otimes \mathcal{H}_C$  and the walk is performed by  $T$  times successive application of the evolution operator on initial state of the walker

$$|\psi_j\rangle_{Fin} = \hat{U}^T |\psi_j\rangle_{Int} = [\hat{S}\hat{C}]^T |\psi\rangle_{Int}. \quad (5)$$

Inspired by Bell states, in this paper, we consider three classes of initial states given by

$$|\psi_1\rangle_{Int} = (\cos \eta |00\rangle_C + e^{I\phi} \sin \eta |11\rangle_C) \otimes |0\rangle_P, \quad (6)$$

$$|\psi_2\rangle_{Int} = (\cos \alpha |10\rangle_C + e^{I\phi} \sin \alpha |01\rangle_C) \otimes |0\rangle_P, \quad (7)$$

$$\begin{aligned} |\psi_3\rangle_{Int} = & [e^{I\phi} \sin \beta (\cos \alpha |10\rangle_C + \sin \alpha |01\rangle_C) + \\ & \cos \beta (\cos \eta |00\rangle_C + \sin \eta |11\rangle_C)] \otimes |0\rangle_P. \end{aligned} \quad (8)$$

The parameters  $\eta$ ,  $\alpha$  and  $\beta$  of the initial state of the walker specify the amount of entanglement between the two qubits [33].  $\phi$  is a phase factor that separates the interference between coin space's bases of the initial state. In fact, this parameter controls how different sectors of

initial state should interfere with each other through the walk. Note that for  $\phi = 0$  and  $\pi$  with  $\eta = \alpha = \pi/4$  in Eqs. (6) and (7), we obtain the infamous Bell states that are maximally entangled. Eq. (8) is one of the most general initial states for our QW.

Rather independent of the particular choice of the parameters for the coins and initial state of the walker, its wave function will occupy  $2T + 1$  positions. At first glance, it seems that due to the coin (3) and shift operators (4), the walker's wave function mostly would remain at the initial position. This is what was observed in Refs. [25, 26]. Later, we will show that this is not always the case and the walk exhibits significantly different behavior depending on initial state's parameters and rotation angles of coin operator.

Before we proceed, we define a few terms to make the upcoming explanations more clear. Two-peaks-zone corresponds to the case where PDD of the walker in position space has two major peaks in it. Accordingly, Three- and Four-peaks-zone indicate the existence of three and four distinguishable peaks. A Gaussian PDD is called classical like behavior. Complete localization takes place when probability density in a specific position is unit and zero for other positions. The coin operator is made out of two sub-coins. If the rotation angles for these two sub-coins are identical, then both qubits are modified identically through the walk. In contrast, if they are not identical, this indicates that these two qubits are modified at different ratio. We call these two cases *identical sub-coins* and *non-identical sub-coins*, respectively.

### III. EFFECTS OF COIN'S AND INITIAL STATE'S PARAMETERS ON WALK

Let us next consider how the coin and the initial state affect the evolution of the walk. To this end, we consider two cases of identical sub-coins ( $\theta = \gamma$ ) and non-identical ones ( $\theta \neq \gamma$ ). For both cases, the walk is analyzed for the initial states given in Eqs. (6) - (8). In section IIIC, we discuss how the obtained results can be interpreted from a physics viewpoint. We limit our study to  $\eta, \theta, \phi, \alpha, \beta \in [0, \pi/2]$ .

#### A. Identical sub-coins: $\theta = \gamma$

For initial state of Eq. (6), the results are given in Fig. 3a. The Three-peaks-zone is observed for PDD. Left (right) hand side peak is an increasing (decreasing) function of the  $\eta$ . The central peak becomes maximum at  $\eta = \pi/4$  where symmetrical PDD is also obtained. Evidently, the symmetry of PDD is only determined by  $\eta$  (see up panel in Fig. 3a). The phase factor,  $\phi$ , has relatively very insignificant effect on probability density in each position (see middle panel in Fig. 3a). The variance of the walk is only  $\theta$  dependent. One can organize the effects of coin parameter,  $\theta$ , into following categories (see down

panel in Fig. 3a): *I*) For  $\theta = \pi/2$ , the PDD is completely localized at one position. When  $\theta \rightarrow \pi/2$ , the walker shows a classical like behavior, i.e. a Gaussian distribution is observed. *II*) If the rotation angle decreases more, it results into: first formation of Three- and then Four-peaks-zone, increments in the variance and amplitudes of extreme zones' peaks, and decrement in amplitude of the central peak. *III*) For  $\theta \rightarrow 0$ , the Four-peaks-zone is modified into Two-peaks-zone and at  $\theta = 0$ , the PDD becomes equally localized in two different positions at extreme zones.

For initial state of Eq. (7), the results are given in Fig. 3b. Surprisingly, contrary to previous case, the symmetry of distribution is not affected by  $\alpha$  and only the probability density at each position is modified by it (see up panel in Fig. 3b). The central peak is minimized (maximized) at  $\alpha = \pi/4$  ( $\alpha = 0$  and  $\pi/2$ ). The phase factor,  $\phi$ , has effects similar to previous case, though more significantly (see middle panel in Fig. 3b). Similar to previous case, the variance of PDD is determined by coin parameter,  $\theta$  and one can observe that (see down panel in Fig. 3b): *I*) For  $\theta = \pi/2$ , the PDD is completely localized at one position (similar to previous case). Contrary to previous initial state, Two-peaks-zone are formed for  $\theta \rightarrow \pi/2$ . *II*) By decreasing  $\theta$  more, the Three- and Four-peaks-zone are observed periodically while the central peak(s) becomes sharper and extreme zones' peaks become smaller. *III*) When  $\theta \rightarrow 0$ , the PDD starts to localize at the central peak and finally complete localization at a single position takes place for  $\theta = 0$  (contrary to previous).

For initial state of Eq. (8), the results are given in Fig. 5a. The symmetry of the distribution is only a function of  $\eta$  and  $\phi$ , and symmetrical PDD is obtained for  $\phi = \pi/2$  and  $\eta = \pi/4$ . The left (right) hand side probability densities are increasing (decreasing) functions of  $\eta$  and  $\phi$ . The central peak becomes minimum at  $\alpha = \pi/4$  and it is an increasing function of  $\beta$ . The effects of variation in coin parameter could be categorized as: *I*) For  $\theta = \pi/2$ , the complete localization at one position takes place. When  $\theta \rightarrow \pi/2$ , the PDD becomes Gaussian. *II*) In case of  $\theta \rightarrow 0$ , PDD starts to localized in three positions and finally it is done at  $\theta = 0$ . *III*) Except for these two cases, Three-peaks-zone are observed with the variance being a decreasing function of  $\theta$ .

As walk proceeds, the variances of PDD increase at the same rate for all the considered initial states (see Fig. 6a). For Eq. (6), the height of three peaks become sharper comparing to the other two initial states. In contrast, the walk with initial state of Eq. (7) has a more homogeneous distribution over position space. In addition, the modification in central peak shows a periodic behavior as a function of steps. The properties of PDD for initial state of Eq. (8) have similarity to other two initial states. This shows that one can understand walks with (6) and (7) initial states as limiting cases of the walk with (8) initial state.

TABLE I: Type of probability density distribution as a function of coin's rotation angle;  $\theta = \gamma$ .

$\theta$	$ \psi_1\rangle_{Int}$	$ \psi_2\rangle_{Int}$	$ \psi_3\rangle_{Int}$
$\theta = 0$	Localized in two positions	Localized in one positions	Localized in three positions
$\theta \rightarrow 0$	Two-peaks-zone	Three-peaks-zone	Three-peaks-zone
$\theta \rightarrow \pi/2$	Gaussian	Two-peaks-zone	Gaussian
$\theta = \pi/2$	Localized in one positions	Localized in one positions	Localized in one positions
Otherwise	Three- and Four-peaks-zone	Three- and Four-peaks-zone	Three-peaks-zone

TABLE II: Type of probability density distribution as a function of coin's rotation angle;  $\theta \neq \gamma$ .

$\theta$	$ \psi_1\rangle_{Int}$	$ \psi_2\rangle_{Int}$	$ \psi_3\rangle_{Int}$
$\theta \rightarrow \pi/2$	Two-peaks-zone	Two-peaks-zone	Two-peaks-zone
$\theta = \pi/2$	Two-peaks-zone	Two-peaks-zone	Two-peaks-zone
$\theta \rightarrow \gamma$	Three-peaks-zone	Three-peaks-zone	Three-peaks-zone
$\theta = \gamma$	Three-peaks-zone	Three-peaks-zone	Three-peaks-zone
Otherwise	Four-peaks-zone	Four-peaks-zone	Four-peaks-zone

### B. Non-identical sub-coins: $\theta \neq \gamma$

In this section, we consider two coins with different rotation angles ( $\theta \neq \gamma$ ). This indicates that entangled qubits building up the coin space are modified differently in each step.

For initial state of (6), the Four-peaks-zone for PDD is observed (see up panel in Fig. 4a), contrary to Three-peaks-zone for previous case. Only  $\eta$  determines the symmetry of distribution (similar to previous case). The amplitudes of the left (right) hand side probabilities are increasing (decreasing) functions of the this parameter. The symmetrical distribution is obtained for  $\eta = \pi/4$ . The phase factor,  $\phi$ , also changes the probability densities but not as significantly as  $\eta$  does so (see middle panel in Fig. 4a). The differences between two cases of  $\theta = \gamma$  and  $\theta \neq \gamma$  become considerably evident by studying the effects of coin's parameters (compare down panels in Figs. 3a and 4a). The first issue is that the classical distribution and complete localization are not seen here. In general, three types of behaviors are seen for the walker (by fixing  $\gamma$  and varying  $\theta$ ): I) Two-peaks-zone which is observed for  $\theta \rightarrow \pi/2$  and  $\theta = \pi/2$ . II) Three-peaks-zone that takes place when  $\theta \rightarrow \gamma$  and  $\theta = \gamma$ . III) Four-peaks-zone which happens for other values of coin parameter and the largest amplitudes for probabilities belong to outer left and right hand side positions.

As for initial state of (7) (see Fig. 4b), the symmetry of PDD is now  $\alpha$  dependent (in contrast to the case of  $\theta = \gamma$ ) and symmetrical PDD is obtained for  $\alpha = \pi/4$ . The phase factor, similar to previous cases, only changes the amplitudes of PDD at each position and it does not affect the symmetry or variance of the distribution (see middle panel in Fig. 4b). As for variation in rotation angle  $\theta$  while  $\gamma$  is fixed, the three behaviors that were reported for initial state of (6) with  $\theta \neq \gamma$ , are also seen

in the same ranges of rotation angles. But there are two noticeable differences: I) The PDD for initial state of (7) is more homogeneous comparing to (6) (compare down panels in Figs. 4a and 4b). II) In case of Four-peaks-zone, the inner peaks have the largest probability densities.

In case of (8) (see Fig. 4b), interestingly,  $\eta$ ,  $\alpha$  and  $\phi$  affect the symmetry of wave function of the walker. The symmetrical PDD is obtained for  $\alpha = \eta = \pi/4$  and  $\phi = \pi/2$  (see Fig. 5b). On the other hand,  $\beta$  only changes the amplitudes of the probability at each position while  $\theta$  determines the variance of the distribution and its type (being Four-peaks-zone or else).

In order to investigate the effects of step numbers, here, we have considered three cases with different  $\gamma$  (see Fig. 6b). The variance of PDD is an increasing function of the step numbers irrespective of choices for initial state. For sufficiently small  $\gamma$ , Four-peaks-zone takes place in which between the inner peaks, probability density is almost zero. This region of zero-probability-density is an increasing function of the steps. Interestingly, it is possible that Three-peaks-zone PDD changes into Four-peaks-zone one by increasing the number of steps. This happens for  $\gamma \rightarrow \theta$  (see middle panels in Fig. 6b).

### C. Discussion on physical interpretation of results

Here, we discuss the results that were obtained in previous sections in more details. Before that, we explain the physical interpretation of each parameter in our setup.

$\eta$  and  $\alpha$  determine the amount of entanglement between the entangled qubits and are among the controlling factors for tuning the entanglement through the walk. In general, the entanglement between these qubits become maximum when  $\eta = \alpha = \pi/4$ . In addition, these two parameters specify the weight of each coin space bases in the



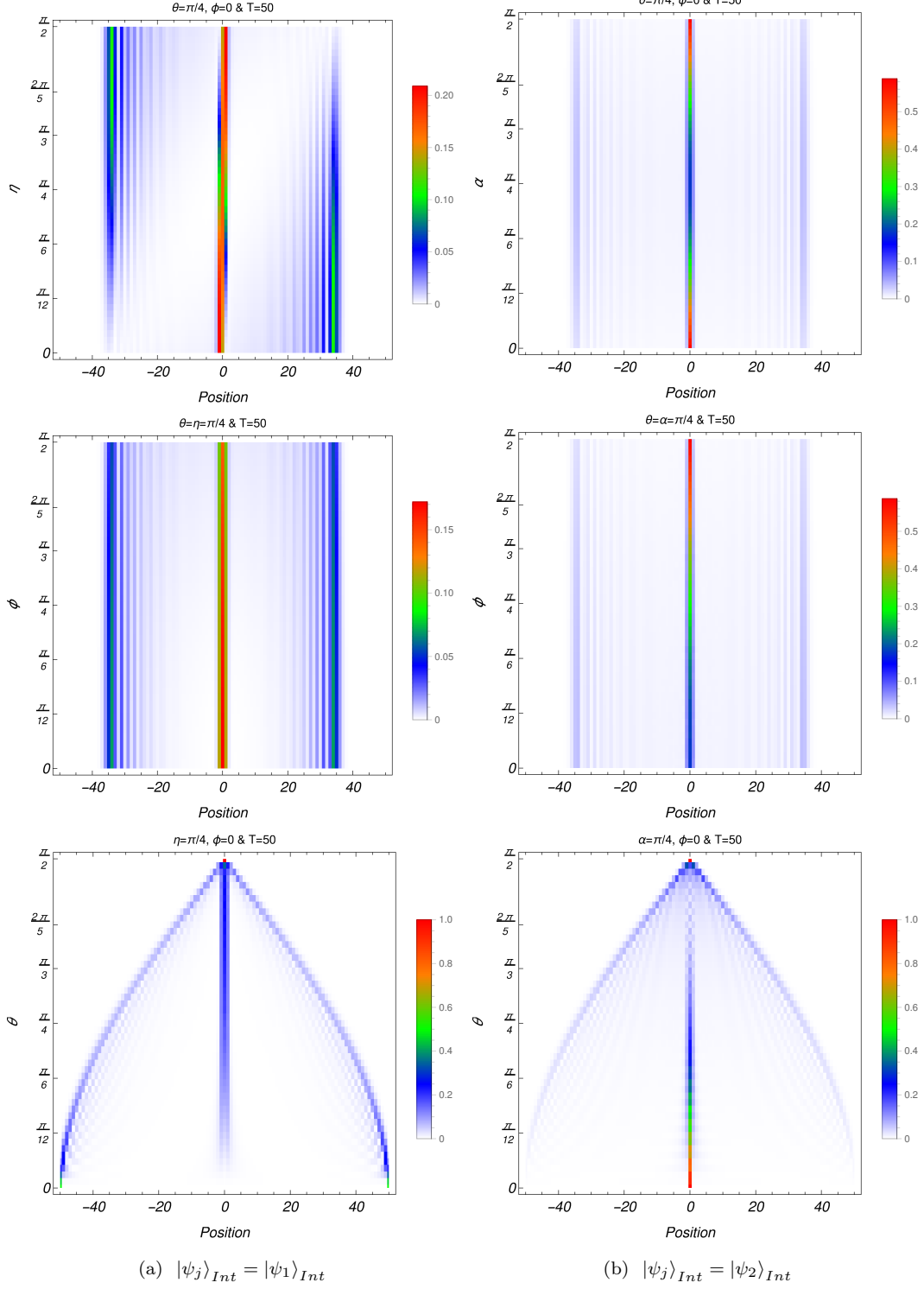


FIG. 3: Probability density versus position for  $T = 50$  steps;  $\theta = \gamma$ .

evolution of walk. The phase factor,  $\phi$  isolates the evolution of one coin space base from the other ones and omit interference between them. In Eqs. (6) - (8), the complete isolation (interference) takes place when  $\phi = \pi/2$  ( $\phi = 0$ ). The rotation angles,  $\theta$  and  $\gamma$  characterize the

coin operator. In one-dimensional QW with a single-qubit coin, the unbiasedness/biasedness of a walk is decided by coin's parameter. For example, the walk with Hadamard coin is considered as unbiased one.

The coin parameters determine how the entangled

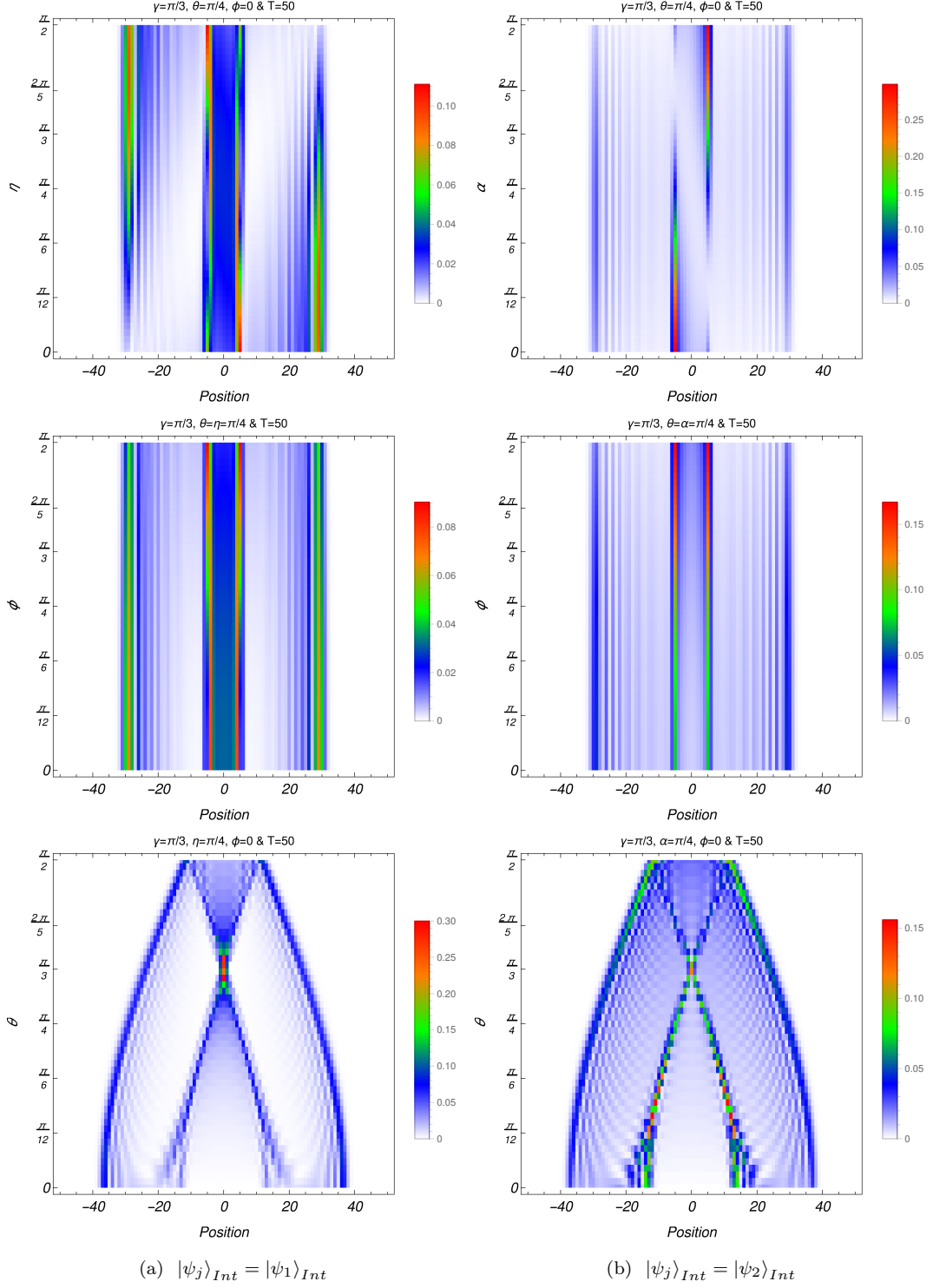


FIG. 4: Probability density versus position for  $T = 50$  step;  $\theta \neq \gamma$ .

qubits would be modified through the walk. When  $\theta = \gamma$ , both qubits are modified identically. Such consideration resulted into diverse distributions for the walker's wave function where the classical like behavior is the least expected (see table I). Previously, it was pointed out that

classical like behavior in QW could be obtained by introduction of decoherence into walk [28–34] or using a step-dependent coin [35]. Here, we see that using two entangled coins is an additional method to simulate classical like behavior. It should be noted that in case of

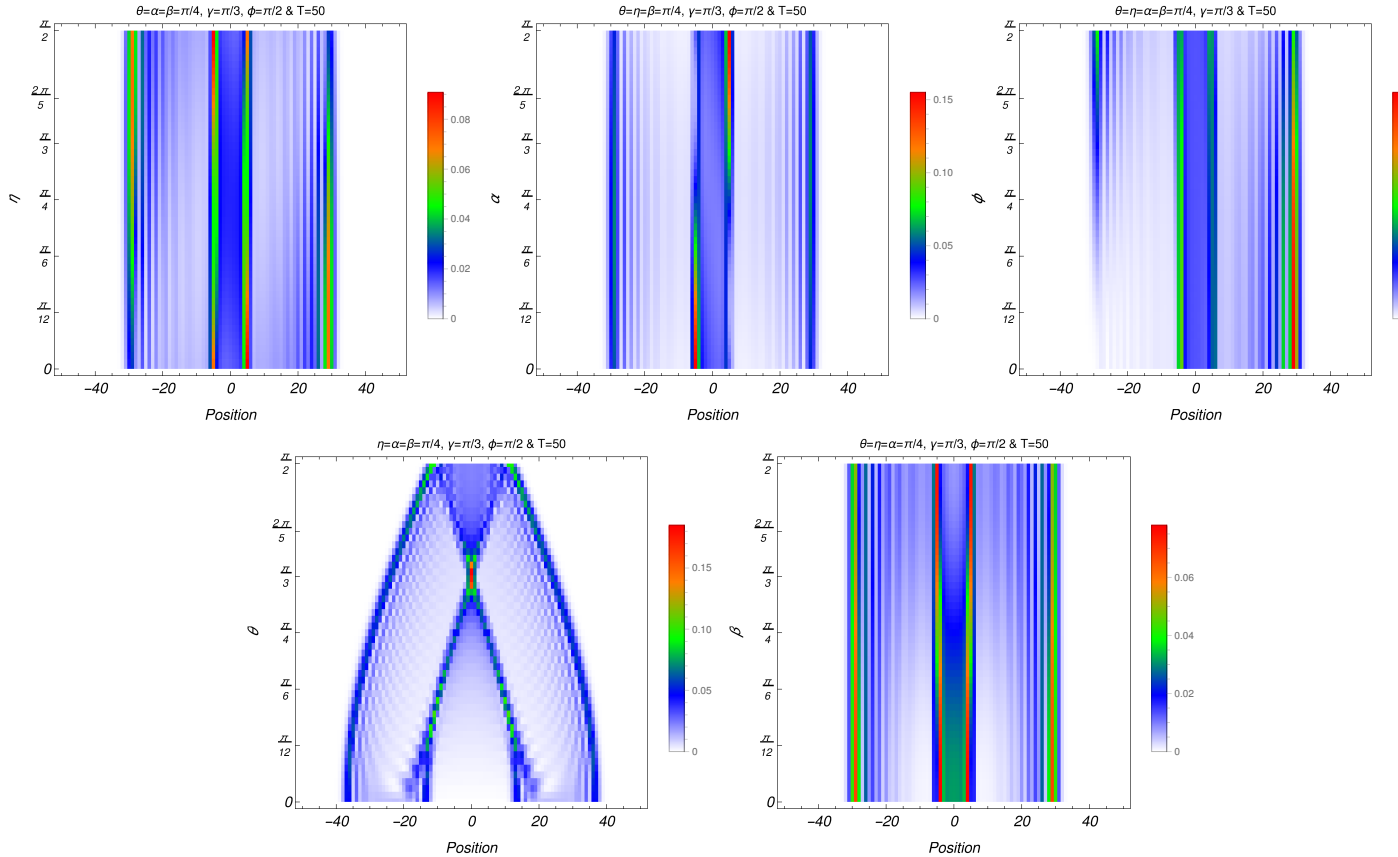
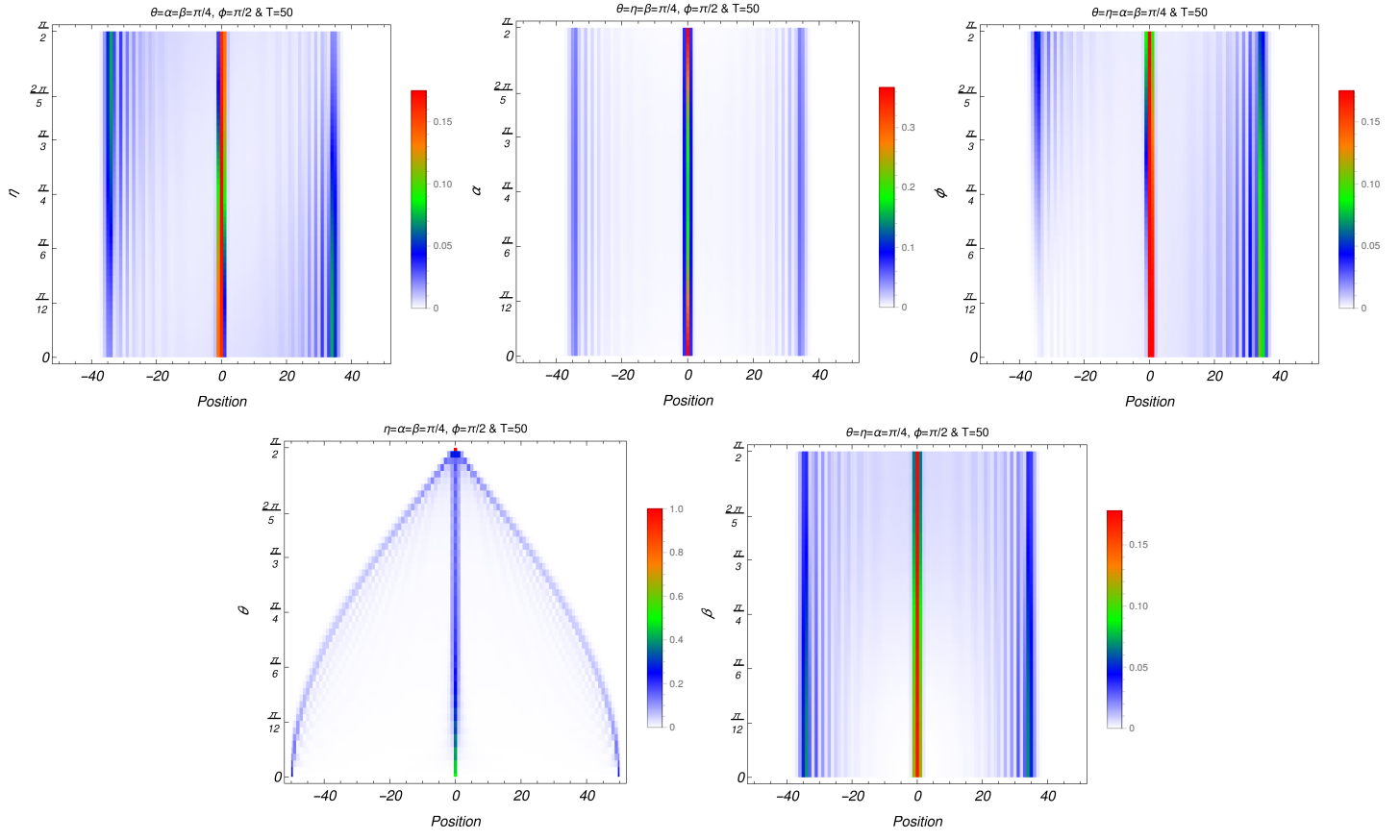
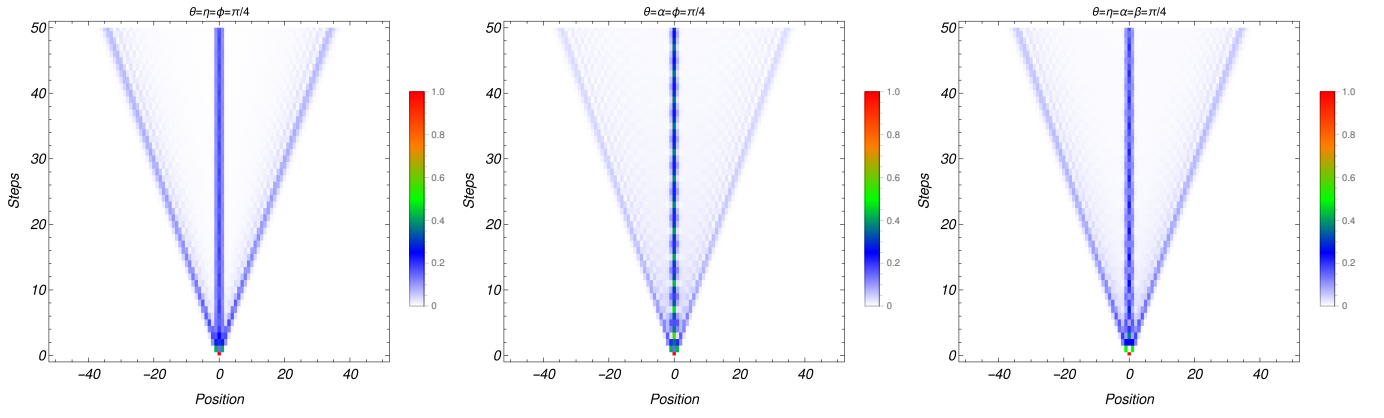
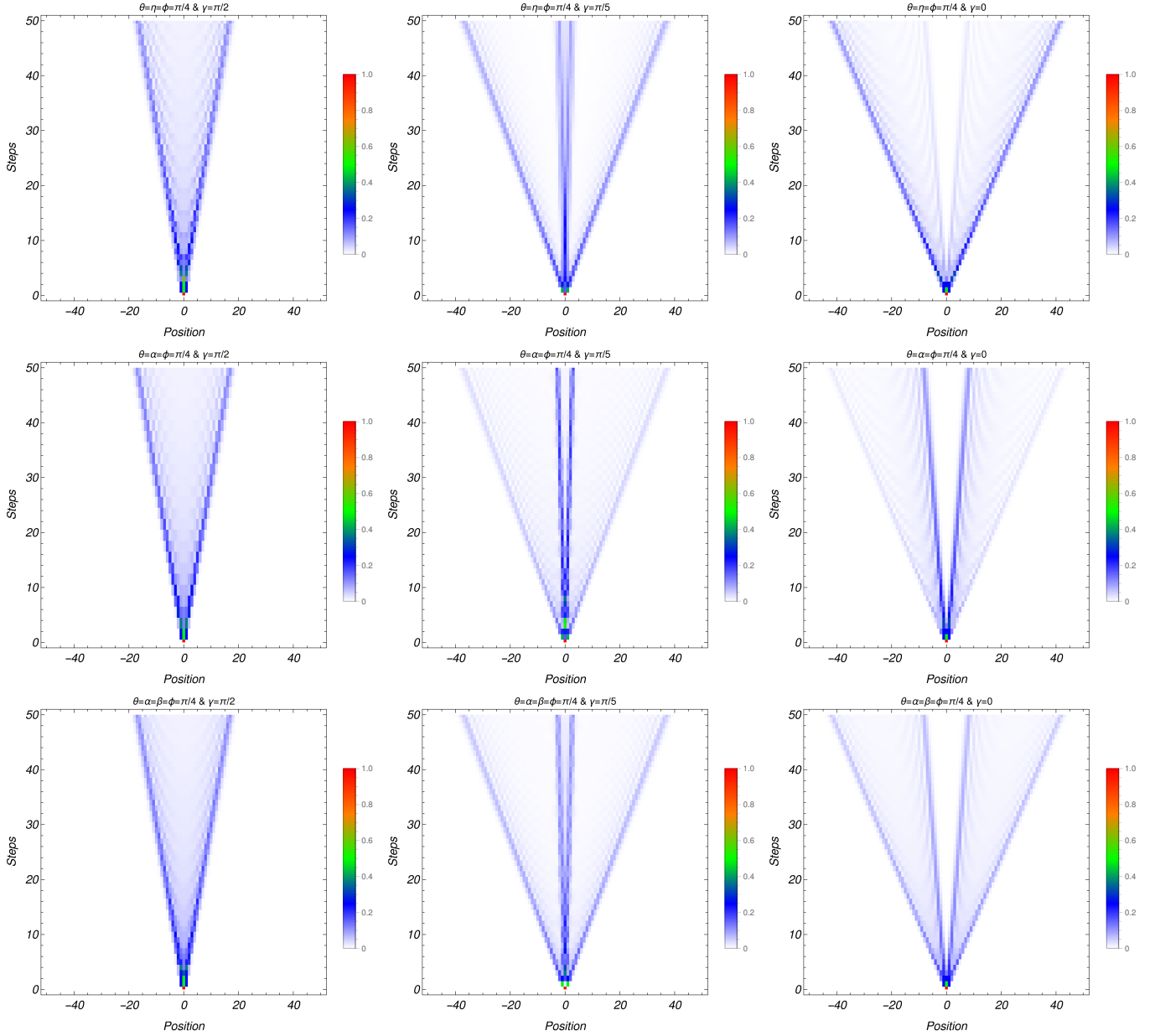


FIG. 5: Probability density versus position for  $T = 50$  step and  $|\psi_j\rangle_{Int} = |\psi_3\rangle_{Int}$ .



(a) For  $\theta = \gamma$ ; **Left:**  $|\psi_j\rangle_{Int} = |\psi_1\rangle_{Int}$ . **Middle:**  $|\psi_j\rangle_{Int} = |\psi_2\rangle_{Int}$ . **Right:**  $|\psi_j\rangle_{Int} = |\psi_3\rangle_{Int}$ .



(b) For  $\theta \neq \gamma$ ; **Up:**  $|\psi_j\rangle_{Int} = |\psi_1\rangle_{Int}$ . **Middle:**  $|\psi_j\rangle_{Int} = |\psi_2\rangle_{Int}$ . **Down:**  $|\psi_j\rangle_{Int} = |\psi_3\rangle_{Int}$ .

FIG. 6: Probability density versus position for subsequent steps  $T = 0.50$ .

decoherence, the classical behavior is obtained when entanglement between coin and position spaces is omitted. Whereas here, the entanglement is used to obtain such behavior. The Two-peaks-zone is similar to usual one-dimensional walk with two internal degrees of freedom. The Three-peaks-zone is also reported for walks with strong decoherence [34] or with step-dependent coin [35]. The Four-peaks-zone is uniquely observed for our setup considered in this paper and is one of the characterization of walk with two entangled qubits. As the sub-coins become different ( $\theta \neq \gamma$ ), the walker's behavior modifies significantly. The first noticeable difference is the absence of classical like behavior and complete localization in walker's PDD (compare tables I and II). The second issue is that Four-peaks-zone is dominant type of distribution. The type of PDD (Four-peaks-zone or else) is specified by the coin's parameters. Even when the number of the steps changes the type, it highly depends on coin's parameters. The independency of type of distribution from initial state's parameters shows that: the Four-peaks-zone and other types are originated from two entangled qubits but they are independent of amount of their initial entanglement. Once again, we highlight the fact that variance of the PDD only depends on coin's parameter. Therefore, mixing and hitting times are determined by coin operator of the walk and for applications such as development of algorithms, the coin plays major role [36, 37]. Finally, the walker's PDD shows more deterministic nature with larger variance for  $\theta = \gamma$ . This is because that despite the distribution in wave function, most of the probability density is concentrated in limited number of the positions (depending on being Two-peaks-zone or else). Whereas, for  $\theta \neq \gamma$ , we have a more homogeneous distribution which is obtained at the cost of smaller variance in PDD (compare Figs. 3 and 4).

Although coin's parameters modify the walker's type of distribution, the symmetry of PDD is independent of it and it only depends on the initial state's parameters. But, such dependency itself depends on two factors: I) What bases are used for the initial state. II) Whether the coin parameters are identical or not. Let us expand on these two factors in more details.

**Identical sub-coins** ( $\theta = \gamma$ ): If the initial state is given only by  $|10\rangle_C$  and  $|01\rangle_C$ , its parameters play no role in determining the symmetry of walker's PDD. They only change the amplitudes of probability density at each position (see Fig. 3b). Therefore, the amount of entanglement between the qubits does not have any effect on the symmetry of walk. It only specifies where the walker's is more probable to be found. In contrast, when the initial state is given only with  $|00\rangle_C$  and  $|11\rangle_C$ , the amount of entanglement plays crucial role in symmetry of the walk and which position holds the highest probability for the walker to be found in (see Fig. 3a). Interestingly, the symmetrical PDD is obtained when entanglement is maximum ( $\eta = \pi/4$ ). The maximization of entanglement has another effect: the most probable place to find the walker is in the starting position, hence,

$|0\rangle_P$ . If we start the walk in the superposition of all four bases, the evolutions of  $|10\rangle_C$  and  $|01\rangle_C$  starts to mix up with  $|00\rangle_C$  and  $|11\rangle_C$ . This results into non-symmetrical PDD. To avoid this, the interferences between these two set of bases should be eliminated. This is done by tuning up the phase factor  $\phi$  to  $\pi/2$ . The second condition for symmetrical PDD is that the bases  $|00\rangle_C$  and  $|11\rangle_C$  must have the same weight ( $\eta = \pi/4$ ). Interestingly, such condition is not seen for  $|10\rangle_C$  and  $|01\rangle_C$  bases (see Fig. 5a). Therefore, maximum entanglement is not a necessary condition for having symmetrical PDD.

**Non-identical sub-coins** ( $\theta \neq \gamma$ ): In this case, the entanglement of initial states (6) and (7) becomes a determining factor for having symmetrical PDD, and this is done when entanglement is maximized ( $\eta = \alpha = \pi/4$ ). Contrary to previous case, when all four bases are used to give the initial state, the symmetrical distribution is obtained only when entanglement is maximized ( $\eta = \alpha = \pi/4$ ) and the evolutions of  $|10\rangle_C$  and  $|01\rangle_C$  are isolated from  $|00\rangle_C$  and  $|11\rangle_C$  ( $\phi = \pi/2$ ). Using these results, one can draw the following conclusion: the effectiveness of  $|10\rangle_C$  and  $|01\rangle_C$  bases highly depend on how the sub-coins acting on two entangled qubits are given. If the sub-coins are identical, the effects of  $|10\rangle_C$  and  $|01\rangle_C$  bases on specific properties of the walker are omitted. As soon as the sub-coins start to differ,  $|10\rangle_C$  and  $|01\rangle_C$  bases contribute to walker's behavior considerably and impose new conditions for having specific properties for the walk. In fact, if we take a look at Figs. 4b and 5b, we can see that the more homogeneous distribution is seen for and rooted in  $|10\rangle_C$  and  $|01\rangle_C$  bases.

#### IV. EVOLUTION OF ENTROPY

Here, we investigate the modification of entropy present in the state of walker. The goal is to understand the effects of different parameters on walker's properties. This is done by investigating the entropy as a function of number of steps, coin's and initial state's parameters.

##### A. von Neumann entropy

In CW and information theory, the entropy of a discrete PDD is investigated by Shannon entropy [38, 39]. As for quantum physics, the von Neumann approach is usually used. This is because for open quantum systems (non-pure states), the density matrix formalism is employed to study system's evolution. Accordingly, the entropy should also be calculated by the properties of the density matrix. The density matrix at step  $T$  of the walk is given by

$$\hat{\rho}_T = |\psi\rangle_T \langle\psi|. \quad (9)$$

The von Neumann method uses the reduced density matrix,  $\hat{\rho}_T^P = \text{Tr}_C(\hat{\rho}_T)$ , to calculate the entropy of posi-

tion space [40]. The von Neumann entropy at time  $T$  is given by

$$S_T^P = -\text{Tr}(\hat{\rho}_T^P \text{Log} \hat{\rho}_T^P), \quad (10)$$

where for walk under consideration in this paper, it yields

$$S_T^P = -\sum_n P_n \text{Log} P_n, \quad (11)$$

in which,  $P_n$  are eigenvalues of Hermitian matrix with the element  $\hat{\rho}_T^P$ . For pure states, the Shannon and von Neumann entropies become identical. Therefore,  $P_n$  is the probability density of the position  $n$ . The results for initial states of (6) and (7), with two cases of identical and non-identical sub-coins are plotted in Figs. 7 and 8. We do our investigation for  $\eta, \phi, \alpha \in [0, 2\pi]$  and  $\theta \in [0, \pi]$ .

### B. Identical versus Non-identical sub-coins

Overall, the entropy increases as walk proceeds irrespective of choices for initial state and sub-coins being identical or not. The only exceptions are where localization takes place in which the entropy is zero (physically expected). The modifications of entropy as a function of walk's parameters show different properties for two cases of identical and non-identical sub-coins. For more clarification, we discuss them separately.

**Identical coins ( $\theta = \gamma$ ):** For initial state of (6), the entropy shows similar behaviors in odd/even steps (see Fig. 7a). The modification in entropy's behavior is symmetrical with respect to  $\theta = \pi/2$ ,  $\eta = 3\pi/4$  and  $\phi = \pi$ . The maximization in entropy at each step takes place at  $\eta = 3\pi/4$ ,  $\phi = \pi$  and  $\pi/6 \leq \theta \leq \pi/4$ . The minimization of entropy depends more on coin's parameter and observed for  $\theta = 0$  and  $\pi/2$  or  $\theta \rightarrow 0$  and  $\pi/2$ . In case of initial state (7), one can notice that the similarity in entropy's behavior for even/odd steps is not observed (see Fig. 7b). The entropy's behavior is symmetrical with respect to  $\theta = \pi/2$ ,  $\alpha = 3\pi/4$  and  $\phi = \pi$ . In contrast to previous initial state, here, entropy minimizes at  $\eta = 3\pi/4$  and  $\phi = \pi$  whereas it maximizes at  $\eta = \pi/4$  and  $\phi \leq \pi/4$ . As for coin's parameter, the entropy becomes minimum at  $\theta = 0$  and  $\pi/2$  or  $\theta \rightarrow 0$  and  $\pi/2$ , similar to previous case.

**Non-identical coins ( $\theta \neq \gamma$ ):** Here, in case of initial state of (6), the first noticeable issue is the absence of similar behaviors that were reported for even/odd steps in previous case (compare Figs. 7a and 8a). The entropy's modification is symmetrical with respect to  $\eta = 3\pi/4$  and  $\phi = \pi$ , similar to previous case, whereas it is no longer symmetrical for  $\theta = \pi/2$ . The entropy becomes maximum for  $\eta = \pi/4$  and  $3\pi/4$ ,  $\pi/4 \leq \phi \leq 3\pi/4$  and  $\theta < \pi/4$ . The initial state (7) shows significantly different behavior for entropy's properties comparing to case with same initial state and identical sub-coins (compare Figs. 7b and 8b). First of all, the minimum for

entropy is no longer observed for  $\theta = 0$  and  $\pi/2$ . In fact, these two cases present relatively large entropy. Minimization in entropy takes place for  $\alpha = 3\pi/4$ ,  $\phi = \pi$  and  $\pi/4 \leq \theta \leq \pi/2$ . On the other hand, entropy becomes maximum for  $\alpha = \pi/4$ ,  $\phi \leq \pi/2$  and  $0 \leq \theta \leq \pi/4$ .

### C. physical interpretation of results

In QWs, the case  $\theta = \gamma = \pi/4$  is known as unbiased walk [1]. This indicates that in the coin toss, all the coin space bases have same chances. Therefore, one may assume that such coin could result into a more homogeneous PDD and maximizes the entropy. In contrast, we observe that for most of the cases, biased walks have the maximum entropy, though usually unbiased walk has a high value of entropy. In all of our studied cases, the highest value for entropy was found for maximally entangled states (Bell states), but not for all of the Bell states (see Figs. 7a and 7b). Therefore, we see that being maximally entangled for initial state is one of the conditions for having maximum entropy. The rotation angles of coin is the second determining factor for maximizing entropy. In fact, depending on choices for these rotation angles, the maximally entangled initial state could admit a minimum instead of maximum in entropy. Though the entropy is a dynamical quantity as a function of steps, we can approximately state that the maximum entropy is obtained for maximally entangled initial state and coin's with rotations angles around and/or smaller than  $\pi/4$ .

The symmetrical properties of entropy as a function of coin's parameters highly depend on sub-coins being identical or different. In contrast, the symmetries observed for initial state's parameters were same for both cases of identical and non-identical coins. For identical sub-coins, the entropy's behavior was symmetrical with respect to  $\theta = \pi/2$ . This shows a periodic behavior within the range of  $0 \leq \theta \leq \pi$ . In contrast, such symmetry is not seen for non-identical sub-coins within this range. This indicates that periodic range is whether found for larger region of coin's parameter or it is absent for this case. Persistence of symmetry associated to initial state's parameters shows that they are more efficient to be utilized in designing algorithms [2, 5], quantum simulations [4] and setups with quantum information applications. This is because if in experimental setups for these purposes, the sub-coins incidentally become non-identical, the symmetrical properties of initial state's parameters remain valid. On the other hand, the modification in symmetrical properties could be indeed used as a factor to recognize problems in experimental setups. In addition, these differences in symmetrical properties are significantly important when this walk is used for exploring topological phases [8], implementation of quantum circuits [41] and quantum state preparation/engineering [10, 11].

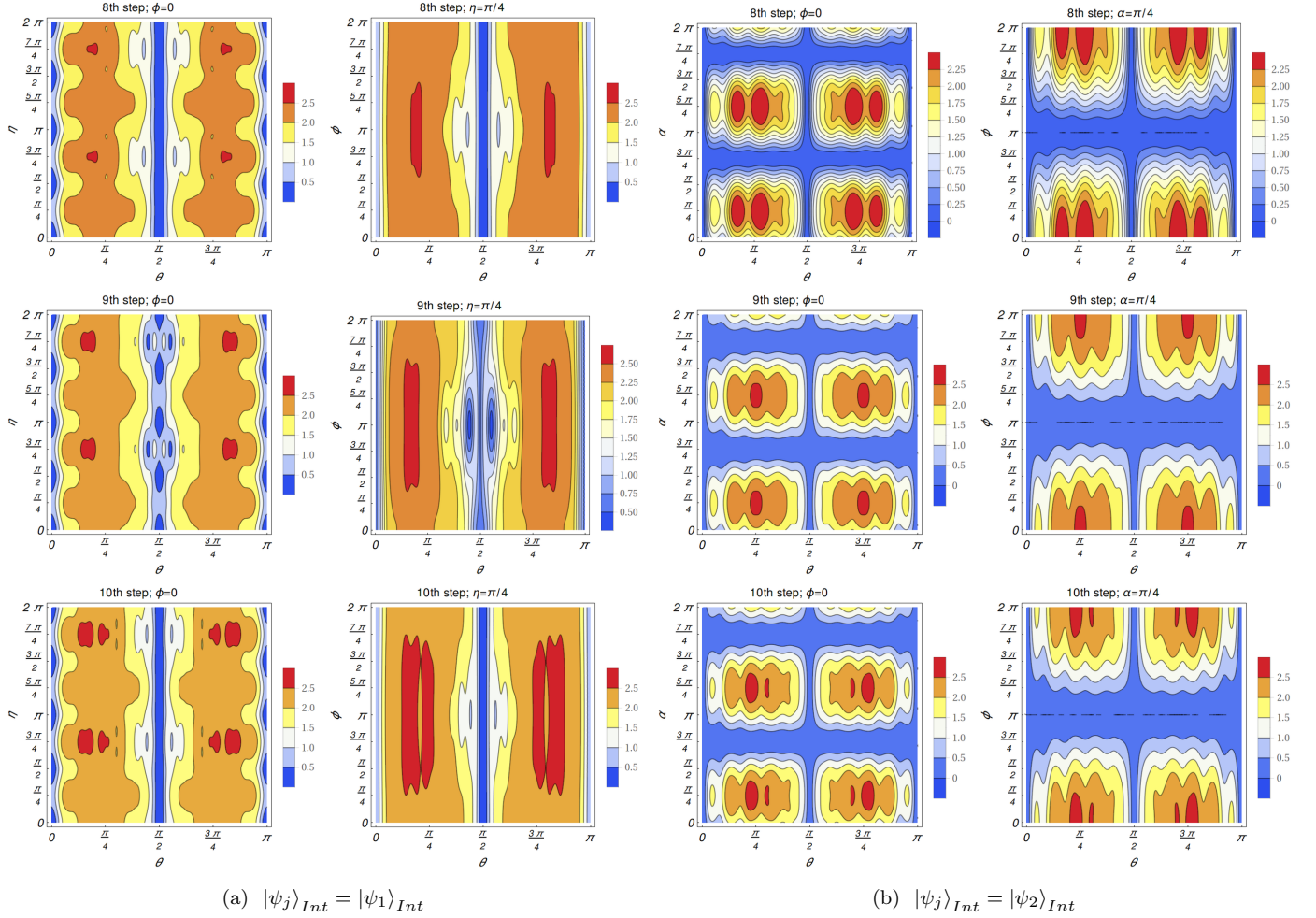


FIG. 7: Entropy as a function of coin's and initial state's parameters for three subsequent steps; for  $\theta = \gamma$ .

## V. CONCLUSION

In this paper, we investigated the one-dimensional QW with four internal degrees of freedom (coin space). The coin space was built up by entanglement of two qubits. The study was done for three distinguishable initial states where for specific values of their parameters, they would yield the infamous Bell states. The coin operator of the walk was made by tensor product of two sub-coins.

The study confirmed that such system or more precisely entanglement between two qubits could be used as a resource for obtaining different PDD in position space including classical like behavior and novel one (Four-peaks-zone). In addition, it was pointed out that properties of walk such as symmetry of PDD, its homogeneity, maximization (minimization) of entropy and amplitudes of probability density in each position are functions of the amount of entanglement in the initial state of the walk. We also showed that the walker's behavior highly depends on the ratio at which entangled qubits are modified. If the ratio of their modifications through walk are

different, the dependency of the walker's properties on initial state's and coin's parameters would change and some specific properties/behaviors are eliminated (for example the classical like behavior). These show that the entangled qubits and the amount of entanglement between them are possible means for state engineering, preparation and quantum simulation.

The importance of our investigation lies within the possibilities that are provided by entanglement in QW. So far, it was shown that entanglement is a unique resource belonging only to quantum systems and absent in classical ones. While the CW is highly celebrated for its applications in different branches of science, for the QW, we indeed have more resources at our disposal. These resources could be utilized for even wider and more applications that their similar ones in CW do not exist. Here, we showed that by introduction of two entangled qubits, we easily cover the classical like behaviors alongside of previously reported ones for QW and obtain even novel ones. Therefore, one can draw the conclusion that entanglement and multi entangled qubit systems for single walker are indeed providing us with more efficient frame-

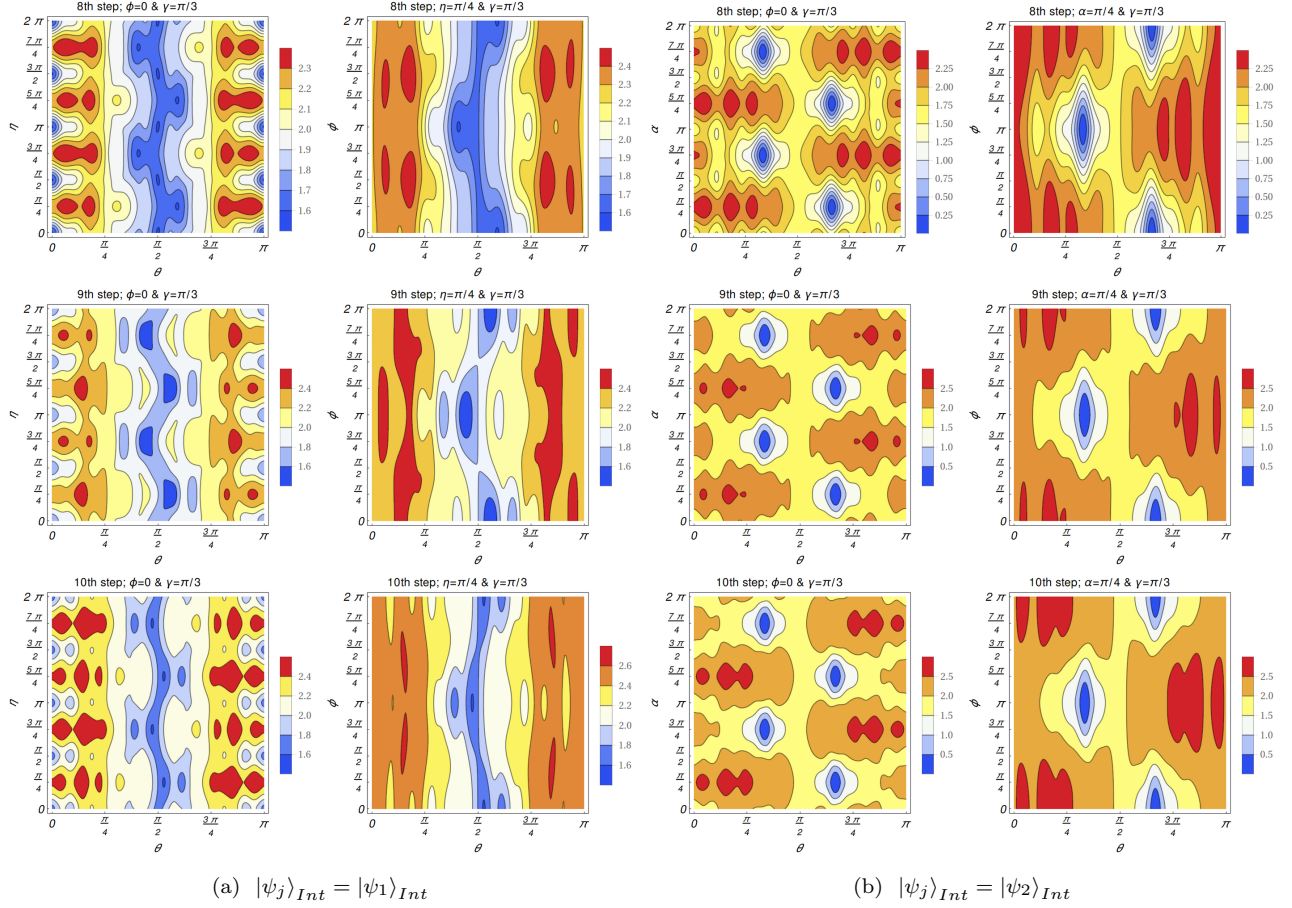


FIG. 8: Entropy as a function of coin's and initial state's parameters for three subsequent steps; for  $\theta \neq \gamma$ .

works comparing to single qubit systems.

### Acknowledgments

SP would like to thank S. Wimberger, S. Barkhofen, and L. Lorz for the helpful comments and discussions.

- 
- |  |  |
|--|--|
| <p>[1] J. Kempe, Contemp. Phys. <b>44</b>, 307 (2003).<br/> [2] N. Shenvi, J. Kempe, and K. B. Whaley, Phys. Rev. A <b>67</b>, 052307 (2003).<br/> [3] A. Ambainis, J. Kempe and A. Rivosh, Proc. 16th ACM-SIAM SODA, 1099, (2005).<br/> [4] M. Mohseni, P. Rebentrost, S. Lloyd and A. Aspuru-Guzik, J. Chem. Phys. <b>129</b>, 174106 (2008).<br/> [5] N. B. Lovett, S. Cooper, M. Everitt, M. Trevers, and V. Kendon, Phys. Rev. A <b>81</b>, 042330 (2010).<br/> [6] M. Montero, Phys. Rev. A <b>95</b> 062326 (2017).<br/> [7] A. Aspuru-Guzik, A. D. Dutoi, P. J. Love and M. Head-Gordon, Science <b>309</b>, 1704 (2005).<br/> [8] T. Kitagawa, M. S. Rudner, E. Berg and E. Demler, Phys. Rev. A <b>82</b>, 033429 (2010).<br/> [9] S. Dernbach, A. Mohseni-Kabir, S. Pal, D. Towsley</p> | <p>and M. Gepner, [arXiv:1801.05417].<br/> [10] C. Di Franco and M. Paternostro, Phys. Rev. A <b>91</b>, 012328 (2015).<br/> [11] L. Innocenti et al Phys. Rev. A <b>96</b>, 062326 (2017).<br/> [12] M. Karski et al, Science <b>325</b>, 174 (2009).<br/> [13] A. Schreiber et al, Phys. Rev. Lett. <b>104</b>, 050502 (2010).<br/> [14] F. Zahringer, G. Kirchmair, R. Gerritsma, E. Solano, R. Blatt and C. F. Roos, Phys. Rev. Lett. <b>104</b>, 100503 (2010).<br/> [15] S. Dadras et al, Phys. Rev. Lett. <b>121</b>, 070402 (2018).<br/> [16] S. Barkhofen, L. Lorz, T. Nitsche, C. Silberhorn and H. Schomerus, [arXiv:1804.09496].<br/> [17] L. Lorz et al, [arXiv:1809.00591].<br/> [18] R. Horodecki et al, Rev. Mod. Phys. <b>81</b>, 865 (2009).<br/> [19] S. Muralidharan and P. K. Panigrahi, Phys. Rev. A</p> |
|--|--|



- 77**, 032321 (2008).
- [20] D. Bouwmeester et al, Nature **390**, 575 (1997).
  - [21] A. K. Ekert, Phys. Rev. Lett. **67**, 661 (1991).
  - [22] R. Jozsa and N. Linden, [arXiv:quant-ph/0201143].
  - [23] F. Hirsch et al, Phys. Rev. Lett. **117**, 190402 (2016).
  - [24] M. Fillettaz, F. Hirsch, S. Designolle, and N. Brunner, Phys. Rev. A **98**, 022115 (2018).
  - [25] S. E. Venegas-Andraca, J. L. Ball, K. Burnett and S. Bose, New J. Phys. **7**, 221 (2005).
  - [26] C. Liu and N. Petulante, Phys. Rev. A **79**, 032312 (2009).
  - [27] C. Liu, Quant. Info. Proc. **11**, 1193 (2012).
  - [28] T. A. Brun, H. A. Carteret and A. Ambainis. Phys. Rev. Lett. **91**, 130602 (2003).
  - [29] J. Kosik, V. Buzek and M. Hillery, Phys. Rev. A **74**, 022310 (2006).
  - [30] V. Kendon, Math. Struct. in Comp. Sci. **17**, 1169 (2006).
  - [31] A. Romanelli, Phys. Rev. A **76**, 054306 (2007).
  - [32] M. Annabestani, S. J. Akhtarshenas and M. R. Abolhasani, Phys. Rev. A **81**, 032321 (2010).
  - [33] S. E. Venegas-Andraca, Quant. Info. Process. **11**, 1015 (2012).
  - [34] A. Alberti, W. Alt, R. Werner and D. Meschede, New J. Phys. **16**, 123052 (2014).
  - [35] S. Panahian and S. Fritzsche, New J. Phys. **20**, 083028 (2018).
  - [36] A. M. Childs and J. Goldstone, Phys. Rev. A **70**, 022314 (2004).
  - [37] M. Santha, [arXiv:0808.0059].
  - [38] C. E. Shannon, The Bell System Technical Journal **27**, 623 (1948).
  - [39] M. A. Nielsen and I. L. Chuang, *Quantum computation and quantum information* (Cambridge University Press, 2010).
  - [40] Y. Ide, N. Konno and T. Machida, Quant. Inf. and Comput. **11**, 855 (2011).
  - [41] X. Qiang et al, Nature Commun. **7**, 11511 (2016).